

Title: LIB-10: ACS Hardware Coordinate Frame Definitions and Transformations	EM Number: GRA-AC-09-0013 Original Release: 6/15/2009 Revision Letter: - Rev 1 Revision Date: - 7/08/2009
Author: R. Olds Phone: 1-9694 Team: ACS	

REFERENCES

- 1.) SIRTf (Spitzer) Reaction Wheel Control Algorithm Description Document (ADD). PCS-100 Rev. A.

CONTENTS

1. INTRODUCTION	2
2. REFERENCE FRAMES	2
2.1 EME-J2000 COORDINATE FRAME {ECI}	2
3. ACS FRAMES	4
3.1 MECHANICAL FRAME {M}.....	4
4. ACS COMPONENT FRAMES AND TRANSFORMATIONS	5
4.1 REACTION WHEEL COORDINATE SYSTEM {RWA}	6
4.2 INERTIAL MEASUREMENT UNIT COORDINATE SYSTEM {IMU}.....	9
4.3 STAR TRACKER COORDINATE SYSTEM {STA}	10
4.4 SUN SENSOR COORDINATE FRAME {SSA}.....	12
5. ACS COMPONENT POSITIONS.....	14
6. THRUSTER ORIENTATIONS.....	15
6.1 ACS THRUSTERS	15
6.1.1 <i>Throat Positions</i>	16
6.1.2 <i>Nozzle Pointing Unit Vectors</i>	17
6.1.3 <i>Thrust Vectors</i>	17
6.2 MAIN ENGINE	18
6.2.1 <i>Throat Position</i>	18
6.2.2 <i>Thruster Nozzle Pointing Unit Vector</i>	18
6.2.3 <i>Thrust Vector</i>	18
7. FUEL TANK	19
8. KA-BAND PAYLOAD.....	19
9. LGA POINTING.....	21
10. REVISION LOG.....	22

1. INTRODUCTION

This document details all the coordinate frames used for the GRAIL mission. The coordinate frames include one inertial reference coordinate frame, one spacecraft body-fixed (mechanical) coordinate frame, and ACS hardware component frames. The transformations between hardware component frames and spacecraft frames are defined in this document. Also included are the mounting locations of the ACS hardware components with respect to the origin of the body-fixed mechanical frame. The thruster positions, thrust vectors, and fuel tank parameters are defined for general reference. Fuel tank data is included to aid fuel slosh analysis. Ka-band payload and LGA pointing unit vectors are also included for reference. All data in this document with the exception of component level coordinate frames and drawings references revision 8 of the GRAIL IDEAS model.

Coordinate Frame Transformation Nomenclature

This document will use the following nomenclature for describing coordinate frame transformations:

$$\vec{v}_B = {}^B_C T \vec{v}_C$$

Where, ${}^B_C T$ = coordinate frame transformation matrix from frame {C} to frame {B}

2. REFERENCE FRAMES

The GRAIL spacecraft will be operated entirely within the Sun/Earth/Moon system from launch to end of mission. For this reason the GRAIL mission uses the EME-J2000 frame as its sole inertial reference frame. There are three flight ephemerides that utilize this reference frame: the Sun ephemeris, Earth ephemeris, and spacecraft/Moon orbital ephemeris. The Sun ephemeris represents the inertial position vector from the Sun to the spacecraft and is relative to the center of the Sun. The Earth ephemeris is also Sun relative and represents the inertial position of the Earth. The orbital ephemeris represents the inertial position of the spacecraft as it orbits the Moon and is taken relative to the center of the Moon (see Figure 2.2).

2.1 EME-J2000 COORDINATE FRAME {ECI}

The Earth-Centered Inertial Coordinate System used by GRAIL is the Earth-Centered Earth Mean Equator and Vernal Equinox of Epoch J2000, also known as the EME, IAU Reference of Epoch J2000, denoted {ECI}. The Epoch J2000 corresponds to the Julian Ephemeris Date (JED) 2451545.0. The axes are defined as follows:

- +X_{ECI} = Parallel to Vernal Equinox of Earth Mean Heliocentric Orbit of Epoch J2000
- +Z_{ECI} = Mean Earth Equator normal of Epoch J2000
- +Y_{ECI} = +Z_{ECI} × +X_{ECI}

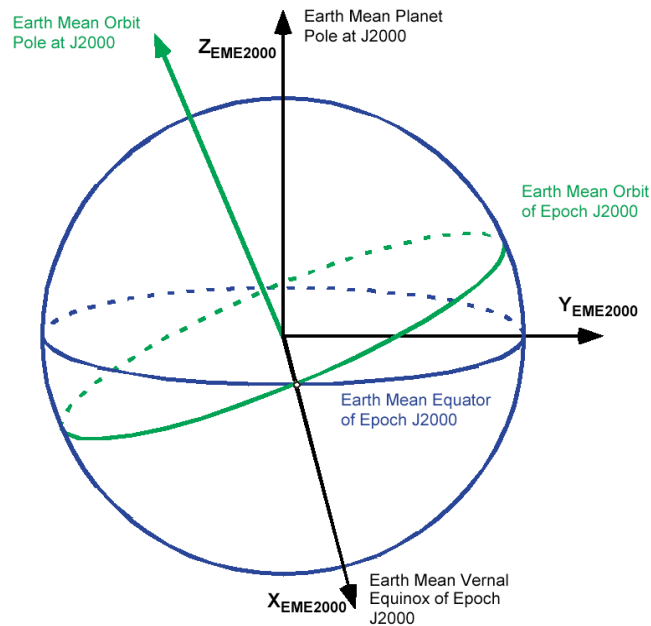


Figure 2.1 - EME-J2000 Inertial Frame (ECI)

During the cruise phase, the spacecraft state is represented by the Sun and Earth ephemerides relative to the center of the Sun, expressed in the EME-J2000 frame (see Figure 2.2, pane A). After LOI, the spacecraft will be captured into lunar orbit and the spacecraft state will be nominally represented by the orbital ephemeris relative to the center of the Moon as depicted in Figure 2.2, pane B.

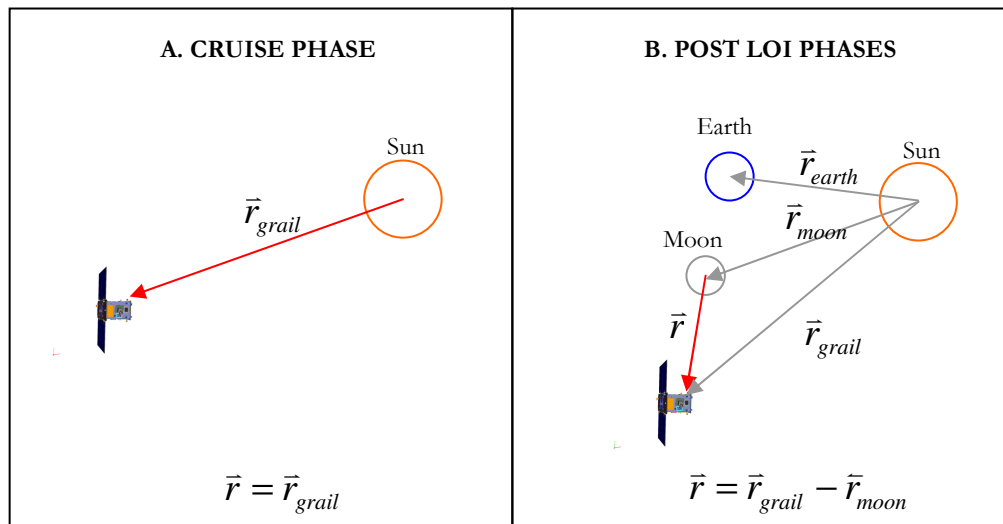


Figure 2.2 - EME-J2000 Reference Bodies

3. ACS FRAMES

There is only one body fixed frame used for the GRAIL spacecraft: Mechanical Frame $\{M\}$. It is important to note that the mechanical frame is identical for both GRAIL-A and GRAIL-B so only a single definition is needed. The mechanical frame acts as a general purpose body fixed frame used both for controlling each of the spacecraft and defining the mounting locations and orientation of the ACS hardware.

3.1 MECHANICAL FRAME $\{M\}$

The origin of the mechanical frame is located on the surface of the $-X$ bus plate and centered in the Y - Z plane (see Figure 3.1 - GRAIL Mechanical $\{M\}$ Frame). The coordinate axes are defined as follows:

- $+X_M$ = Parallel to and in opposite direction of solar array normal
- $+Z_M$ = Normal to bus plate where star tracker is mounted
- $+Y_M = +Z_M \times +X_M$

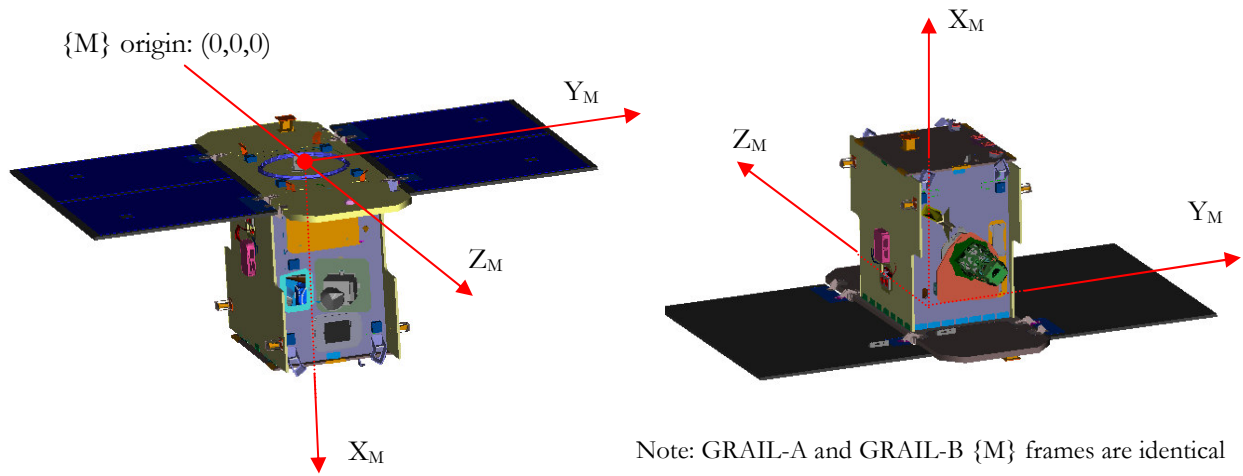


Figure 3.1 - GRAIL Mechanical $\{M\}$ Frame

4. ACS COMPONENT FRAMES AND TRANSFORMATIONS

There are 4 ACS components per spacecraft, each with its individual local coordinate frame:

1. Reaction Wheels (4 per spacecraft)
2. Inertial Measurement Unit (1 per spacecraft)
3. Star Tracker Assembly (1 per spacecraft)
4. Sun Sensor Assembly (1 per spacecraft)

All spacecraft models illustrated herein are taken from revision 8 of the GRAIL IDEAS model.

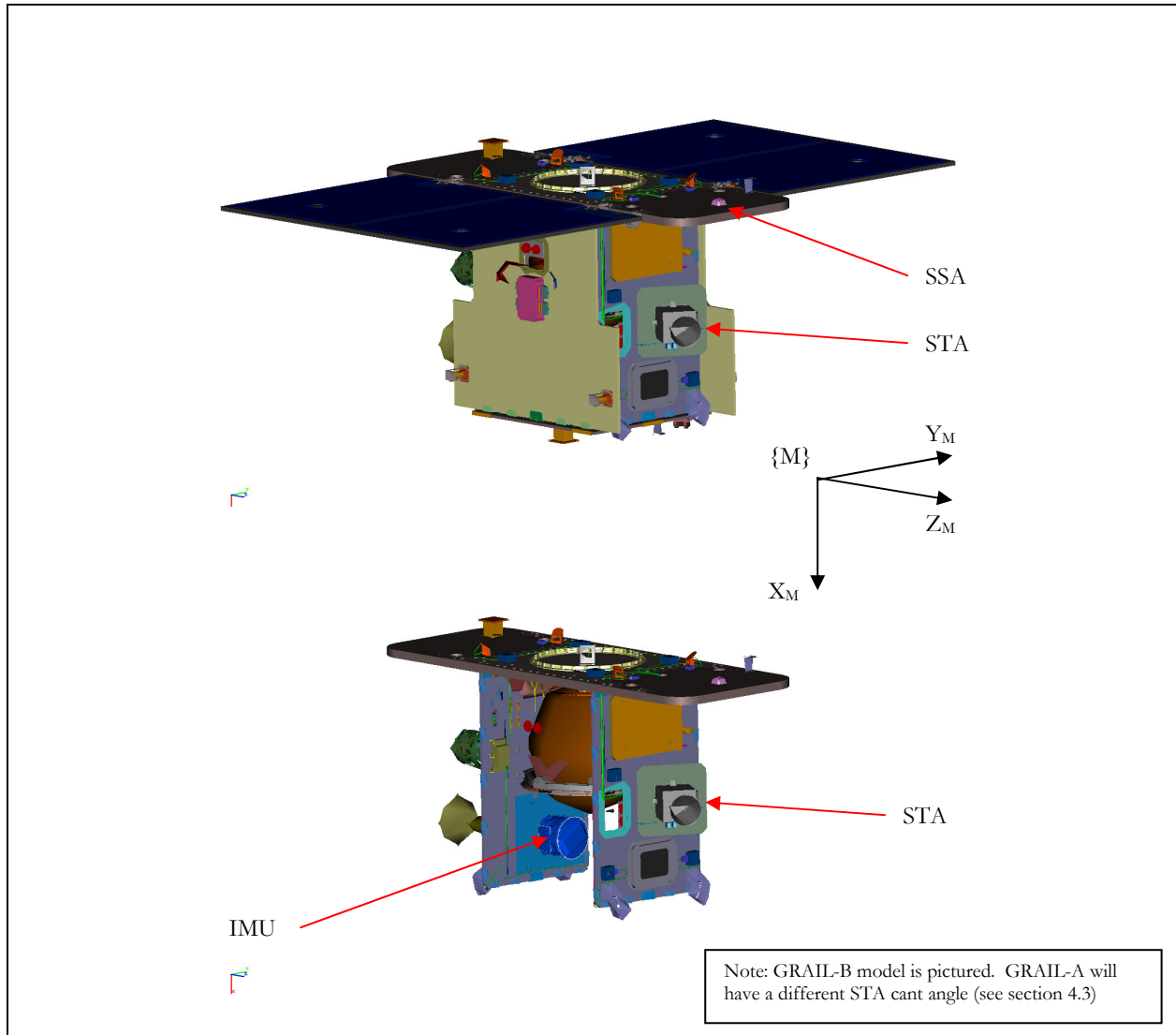


Figure 4.1 - Star Tracker (STA), Inertial Measurement Unit (IMU), and Sun Sensor (SSA) View

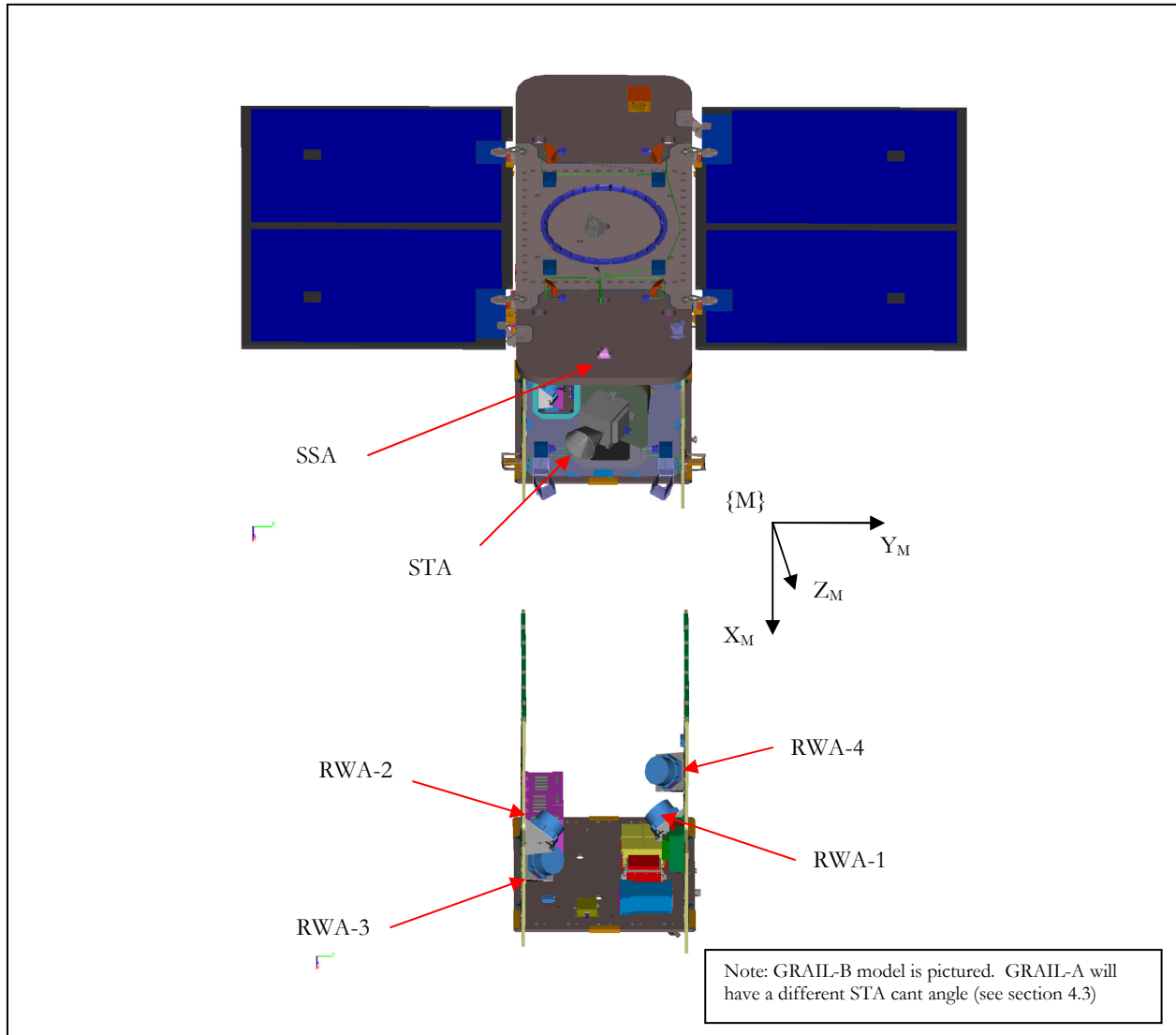


Figure 4.2 - Reaction Wheel (RWA), Star Tracker (STA), and Sun Sensor (SSA) View

Each component reports its associated sensor data in its corresponding local frame. The reaction wheels each apply torque on the spacecraft in their own associated local wheel frame. Each local component coordinate frame is mapped to the mechanical frame for use in the ACS control system. The following subsections provide detailed descriptions of each of the ACS component coordinate frames and list transformations for each to the mechanical frame.

4.1 REACTION WHEEL COORDINATE SYSTEM {RWA}

Each spacecraft houses 4 reaction wheels oriented in a pyramid configuration. The pyramid configuration provides an extra degree of freedom allowing the wheels to be spun up or down in tandem without applying any torque to the spacecraft. The reaction wheel pyramid configuration is described in Figure 4.3. The geometry of this configuration was chosen to provide an equal gain for momentum storage in the y and z axes of the mechanical frame, while also boosting momentum capacity in the x-axis of the mechanical frame for storing momentum due to gravity gradient torques. More momentum storage was devoted to the y and z

body-axes because the dominant external torque due to solar radiation acts in these axes. Gravity gradient torques act primarily in the x-body axis, but are a factor of 3 to 4 less than those of solar torques.

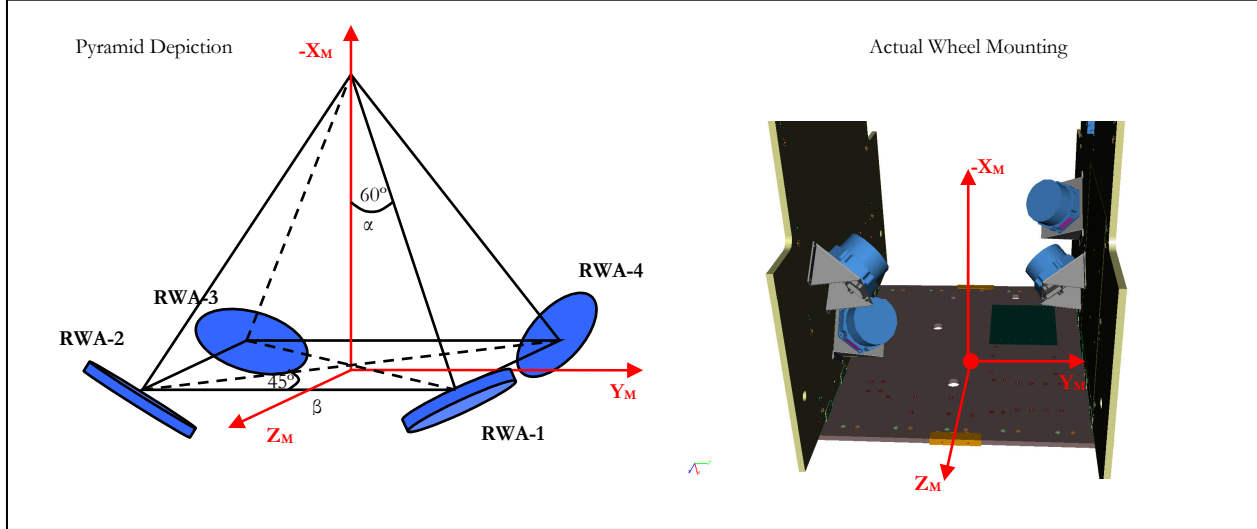


Figure 4.3- 4-Wheel Pyramid Configuration

In the diagram above, the α angle defines the elevation of each wheel spin axis (how steep the pyramid is), while the β angle defines the azimuth of each wheel spin axis. The pyramid configuration with $\alpha = 60$ deg, and $\beta = 45$ deg, increases the capability possible with only a single wheel in each axis by as much as 245% in the y and z axes, and 200% in the x-axis. The pyramid also causes a set of minimum torque axes in the mechanical frame that can only provide 98% the capability of a single wheel.

Figure 4.4 below shows the phasing of each wheel. When viewed from above on the anti-connector side, positive spin is defined as counter-clockwise. When viewed from the connector side, positive spin is defined as clockwise.

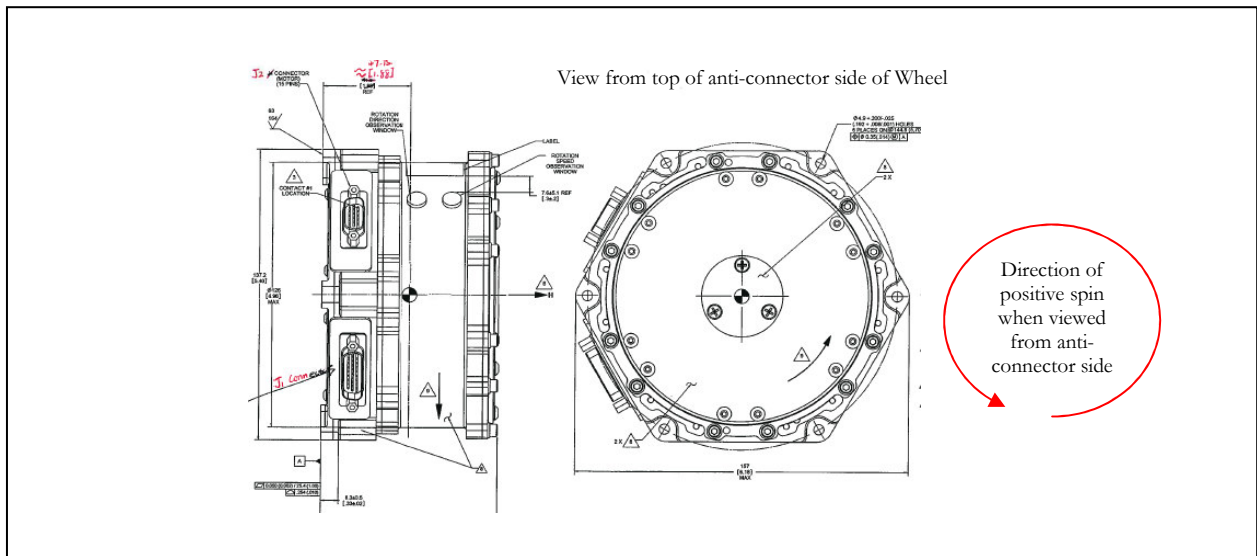


Figure 4.4 - Wheel Local Coordinates and Phasing (schematics taken from Goodrich drawing 45159 rev.2)

The unit vectors for the wheel spin-axes (defined in the body frame) are listed below in Table 4. 1 for $\alpha = 60$ deg, $\beta = 45$ deg. These unit vectors are used to define the columns of the transformation matrix that maps the 4-wheel coordinate system to the spacecraft body axes. This transformation is identical for GRAIL-A and GRAIL-B.

$${}_{RWA}^M T = [\hat{w}_{1b} \quad \hat{w}_{2b} \quad \hat{w}_{3b} \quad \hat{w}_{4b}]$$

$${}_{RWA}^M T = \begin{bmatrix} -\cos(\alpha) & -\cos(\alpha) & -\cos(\alpha) & -\cos(\alpha) \\ -\sin(\alpha)\cos(\beta) & \sin(\alpha)\sin(\beta) & \sin(\alpha)\cos(\beta) & -\sin(\alpha)\sin(\beta) \\ -\sin(\alpha)\sin(\beta) & -\sin(\alpha)\cos(\beta) & \sin(\alpha)\sin(\beta) & \sin(\alpha)\cos(\beta) \end{bmatrix} \quad [\text{Ref. 1}]$$

Table 4. 1 - Reaction Wheel Spin Axis Unit Vectors (Map from 4-wheel coordinates to body axis)

	RWA-1	RWA-2	RWA-3	RWA-4
X	-0.5000	-0.5000	-0.5000	-0.5000
Y	-0.6124	0.6124	0.6124	-0.6124
Z	-0.6124	-0.6124	0.6124	0.6124

The inverse transformation, which maps the spacecraft body axes onto the 4-wheel coordinate system, is defined using the pseudo-inverse of the transformation above.

$${}_{M}^{RWA} T = {}_{RWA}^M T^T \left({}_{RWA}^M T {}_{RWA}^M T^T \right)^{-1}$$

$${}_{M}^{RWA} T = \begin{bmatrix} -1 & -\frac{\cos(\beta)}{4\cos(\alpha)} & -\frac{\sin(\beta)}{2\sin(\alpha)} \\ -1 & \frac{\sin(\beta)}{2\sin(\alpha)} & -\frac{\cos(\beta)}{2\sin(\alpha)} \\ -1 & \frac{\cos(\beta)}{2\sin(\alpha)} & \frac{\sin(\beta)}{2\sin(\alpha)} \\ -1 & \frac{\sin(\beta)}{2\sin(\alpha)} & \frac{\cos(\beta)}{2\sin(\alpha)} \\ -1 & -\frac{\sin(\beta)}{2\sin(\alpha)} & \frac{\cos(\beta)}{2\sin(\alpha)} \\ -1 & \frac{\sin(\beta)}{2\sin(\alpha)} & \frac{\cos(\beta)}{2\sin(\alpha)} \end{bmatrix} \quad [\text{Ref. 1}]$$

Table 4. 2 - Map from body frame to 4-wheel coordinates

	X	Y	Z
RW-1	-0.5000	-0.4082	-0.4082
RW-2	-0.5000	0.4082	-0.4082
RW-3	-0.5000	0.4082	0.4082
RW-3	-0.5000	-0.4082	0.4082

In this orientation, the mapping from the 4-wheel system to the body frame creates an underdetermined system since there are 4 wheels controlling 3 axes in the body frame. This creates a non-zero null space in the transformation defined in Table 4. 1 so that the wheels can be commanded in tandem without imparting any net torque on the spacecraft. The null space is spanned by the 4-vector defined below.

$$\text{null}({}_{RWA}^M T) = [0.5 \quad -0.5 \quad 0.5 \quad -0.5] \quad [\text{Ref. 1}]$$

This shows that if the wheels are commanded to provide equal magnitude torques, with RW-1 and RW-3 being opposite in sign to RW-2 and RW-4, no net torque will be imparted on the spacecraft. This extra degree of freedom is used to avoid zero crossings and increase the momentum capacity of the reaction wheel system.

4.2 INERTIAL MEASUREMENT UNIT COORDINATE SYSTEM {IMU}

The local IMU coordinate frame, which is coincident with the IMU sensing frame, is associated with the physical design of the IMU and defined as follows:

- +Y_{IMU} = Collinear with the outward normal to Y axis alignment mirror (primary mirror), Anti-Normal to J1 and J2 Connectors
- +Z_{IMU} = Perpendicular to the Y axis and in the plane formed by the outward normal of the Y axis mirror and the Z axis mirror (secondary mirror), positive in the outward normal direction.
- +X_{IMU} = +Y_{IMU} × +Z_{IMU}

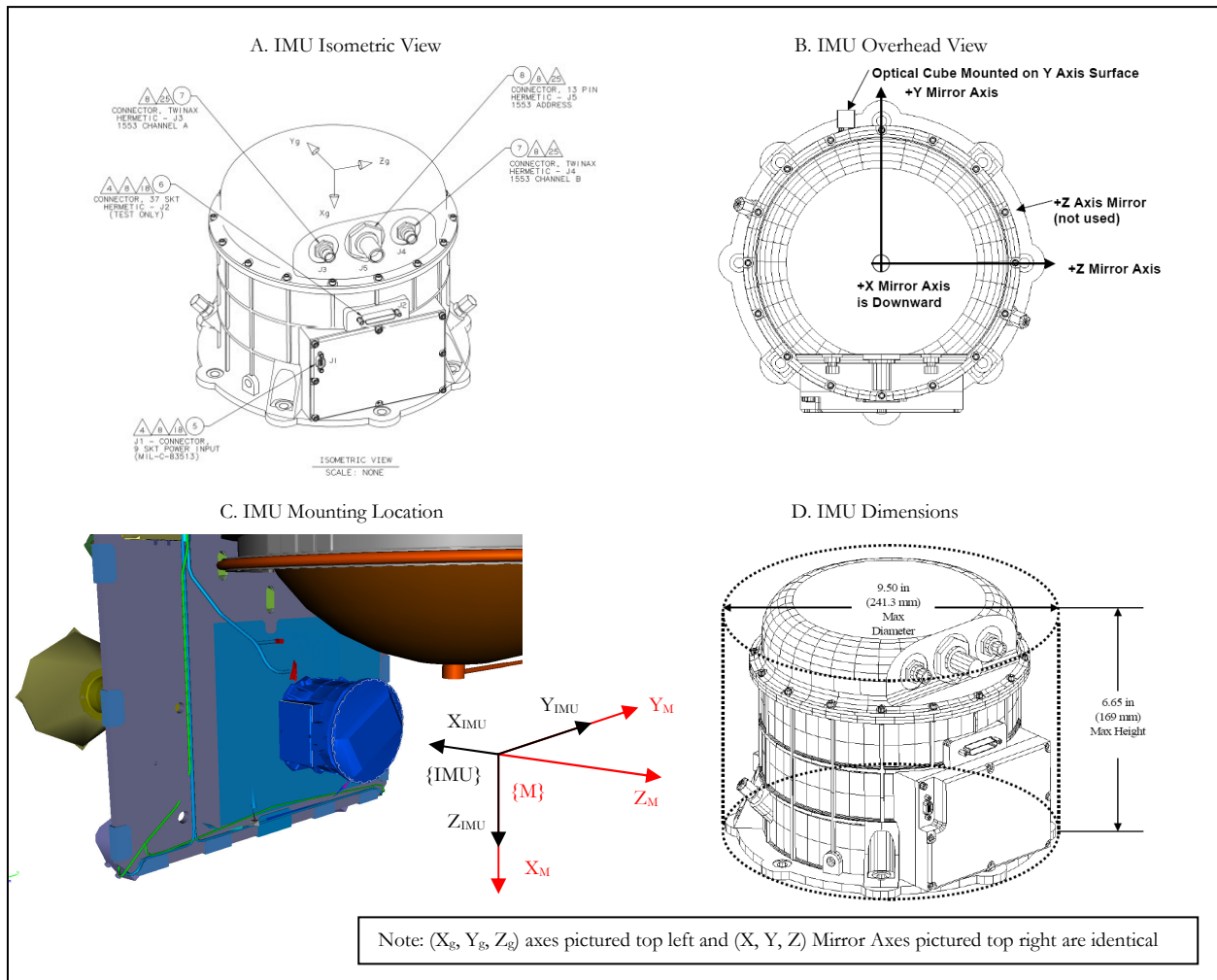


Figure 4.5 - IMU Local Coordinate Frame and Component Views (schematics taken from Honeywell ICD rev. C – June 14, 2004)

The IMU local coordinate frame {IMU} is pictured in Figure 4.5, panes A, B, and C. The {IMU} frame orientation with respect to the {M} frame will be identical in the case of both GRAIL-A and GRAIL-B. The nominal transformation from the {IMU} frame to the {M} frame is below.

$${}_{IMU}^M T = \begin{bmatrix} 0 & 0 & 1 \\ 0 & 1 & 0 \\ -1 & 0 & 0 \end{bmatrix}$$

The nominal transformation from the {M} frame to the {IMU} frame will be the transpose of ${}_{IMU}^M T$:

$${}_{M}^{IMU} T = \begin{bmatrix} 0 & 0 & -1 \\ 0 & 1 & 0 \\ 1 & 0 & 0 \end{bmatrix}$$

4.3 STAR TRACKER COORDINATE SYSTEM {STA}

The star tracker alignment is spacecraft dependent (GRAIL-A or GRAIL-B) since each spacecraft uses a different cant angle for the unit. The unique cant angles are designed so that the tracker for each spacecraft will be pointed away from the Moon while in the science taking attitude (orbiter-to-orbiter pointing) when GRAIL-B is leading the formation and GRAIL-A is following GRAIL-B. Figure 4.6 shows the cant angle for each spacecraft.

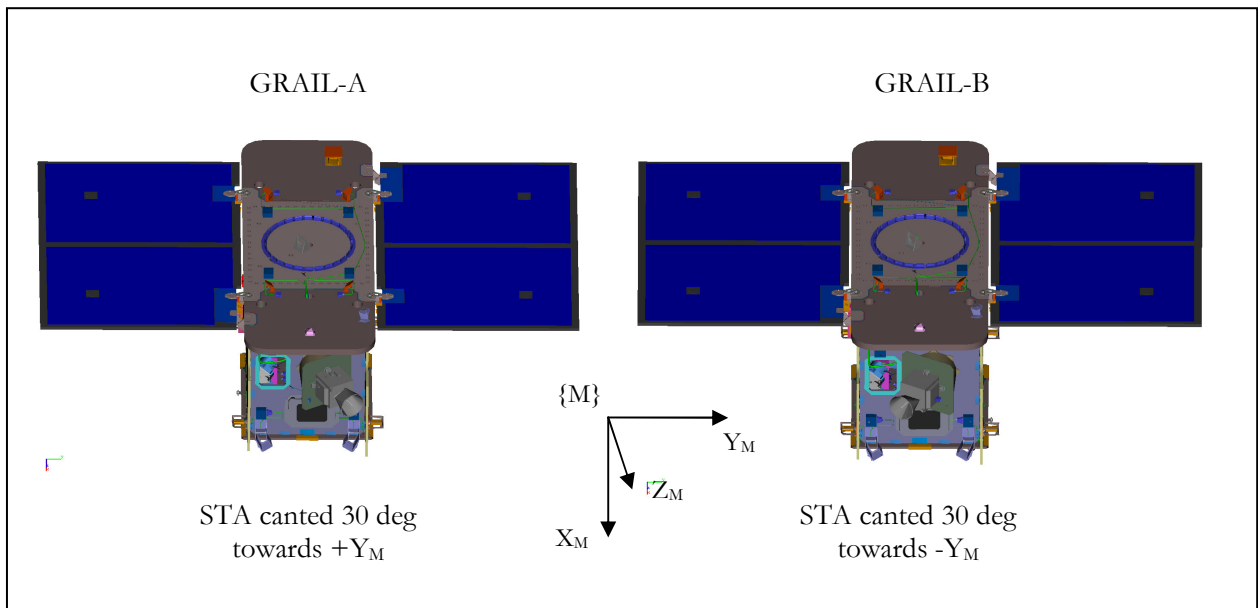


Figure 4.6 - Star Tracker Cant Angle for GRAIL-A and GRAIL-B

The local mechanical star tracker coordinate frame is associated with the physical design of the star tracker and defined as follows (matches the reference frame indicated in Figure 4.7, with the “STA” subscript):

+Z_{STA} = Parallel to tracker bore sight, pointing towards observed sky

$+X_{STA} = \text{Orthogonal to } +Z_{STA}, \text{ and oriented such that the reference cube is in the } +X, -Y \text{ corner of the unit (towards unit electronics)}$
 $+Y_{STA} = +Z_{STA} \times +X_{STA}$

Figure 4.7, pane A illustrates the Star Tracker Local Mechanical Coordinate Frame, viewed from the star's perspective, with the tracker bore sight out of the page:

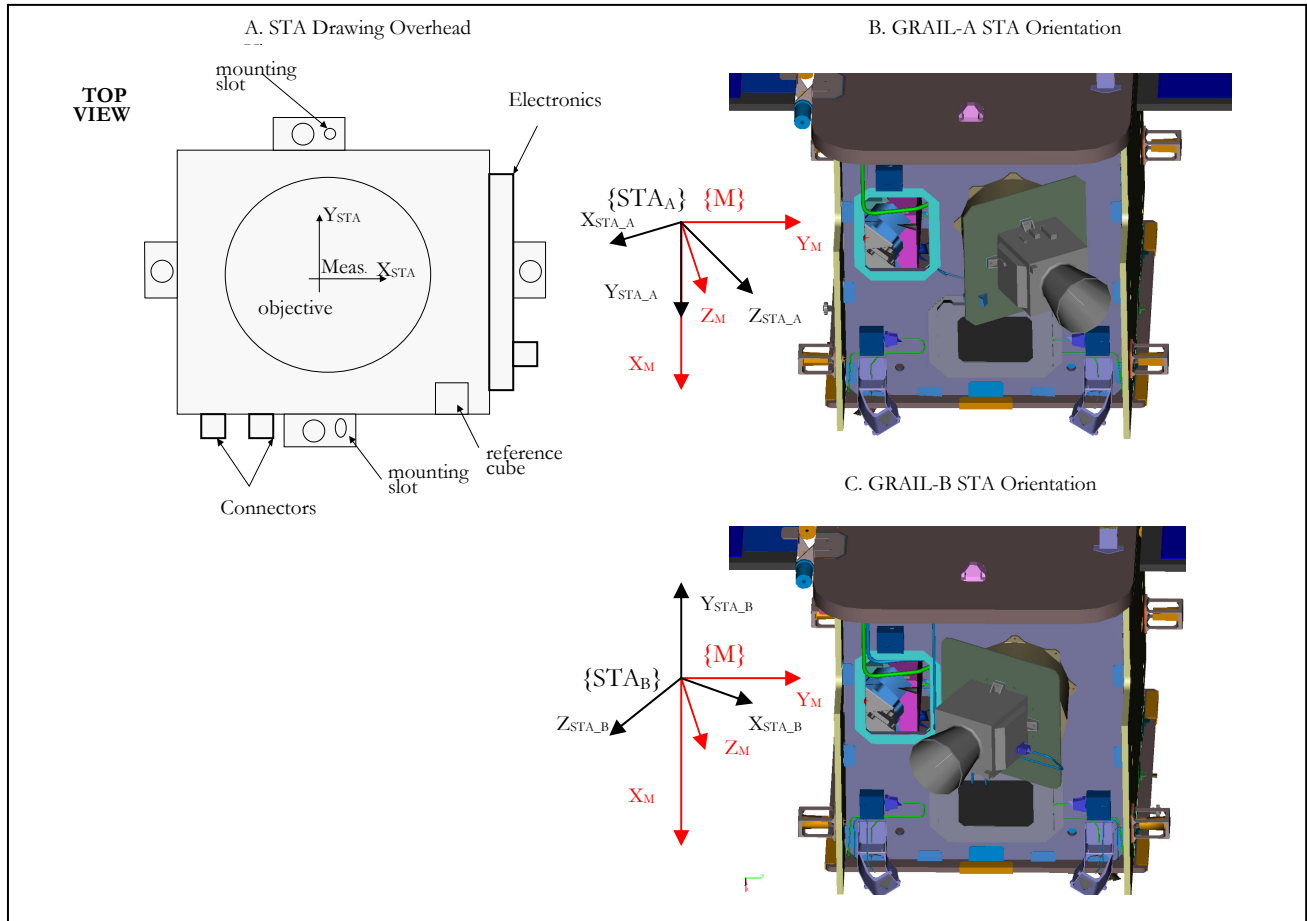


Figure 4.7 - Star Tracker Local Coordinate Frame and Component Views (drawings taken from Phoenix A-STR ICD rev 0, dated 3/31/05)

The nominal coordinate frame transformations from the $\{STA\}$ frame to the $\{M\}$ frame for each spacecraft are below:

$${}_{STA_A}^M T = \begin{bmatrix} 0 & 1 & 0 \\ -\cos(\pi/6) & 0 & \sin(\pi/6) \\ \sin(\pi/6) & 0 & \cos(\pi/6) \end{bmatrix} = \begin{bmatrix} 0 & 1 & 0 \\ -0.86603 & 0 & 0.50000 \\ 0.50000 & 0 & 0.86603 \end{bmatrix}$$

$${}_{STA_B}^M T = \begin{bmatrix} 0 & -1 & 0 \\ \cos(\pi/6) & 0 & -\sin(\pi/6) \\ \sin(\pi/6) & 0 & \cos(\pi/6) \end{bmatrix} = \begin{bmatrix} 0 & -1 & 0 \\ 0.86603 & 0 & -0.50000 \\ 0.50000 & 0 & 0.86603 \end{bmatrix}$$

The nominal transformations from the {M} frame to the {STA} frame for each spacecraft will be the transpose of ${}_{STA_A}^M T$ and ${}_{STA_B}^M T$:

$${}_{M}^{STA_A} T = \begin{bmatrix} 0 & -\cos(\pi/6) & \sin(\pi/6) \\ 1 & 0 & 0 \\ 0 & \sin(\pi/6) & \cos(\pi/6) \end{bmatrix} = \begin{bmatrix} 0 & -0.86603 & 0.50000 \\ 1 & 0 & 0 \\ 0 & 0.50000 & 0.86603 \end{bmatrix}$$

$${}_{M}^{STA_B} T = \begin{bmatrix} 0 & \cos(\pi/6) & \sin(\pi/6) \\ -1 & 0 & 0 \\ 0 & -\sin(\pi/6) & \cos(\pi/6) \end{bmatrix} = \begin{bmatrix} 0 & 0.86603 & 0.50000 \\ -1 & 0 & 0 \\ 0 & -0.50000 & 0.86603 \end{bmatrix}$$

4.4 SUN SENSOR COORDINATE FRAME {SSA}

The local sun sensor assembly coordinate frame is associated with physical design of the sun sensor assembly and is defined as follows. The sun sensor assembly mounting location and coordinate frame transformations are identical for each spacecraft.

$$\begin{aligned} +Y_{SSA} &= \text{Anti-Normal to Connector} \\ +Z_{SSA} &= \text{Parallel to Bore sight} \\ +X_{SSA} &= +Y_{SSA} \times +Z_{SSA} \end{aligned}$$

Figure 4.8 illustrates the local sun sensor assembly coordinate frame and the mounting of the sun sensors with respect to the spacecraft mechanical axes:

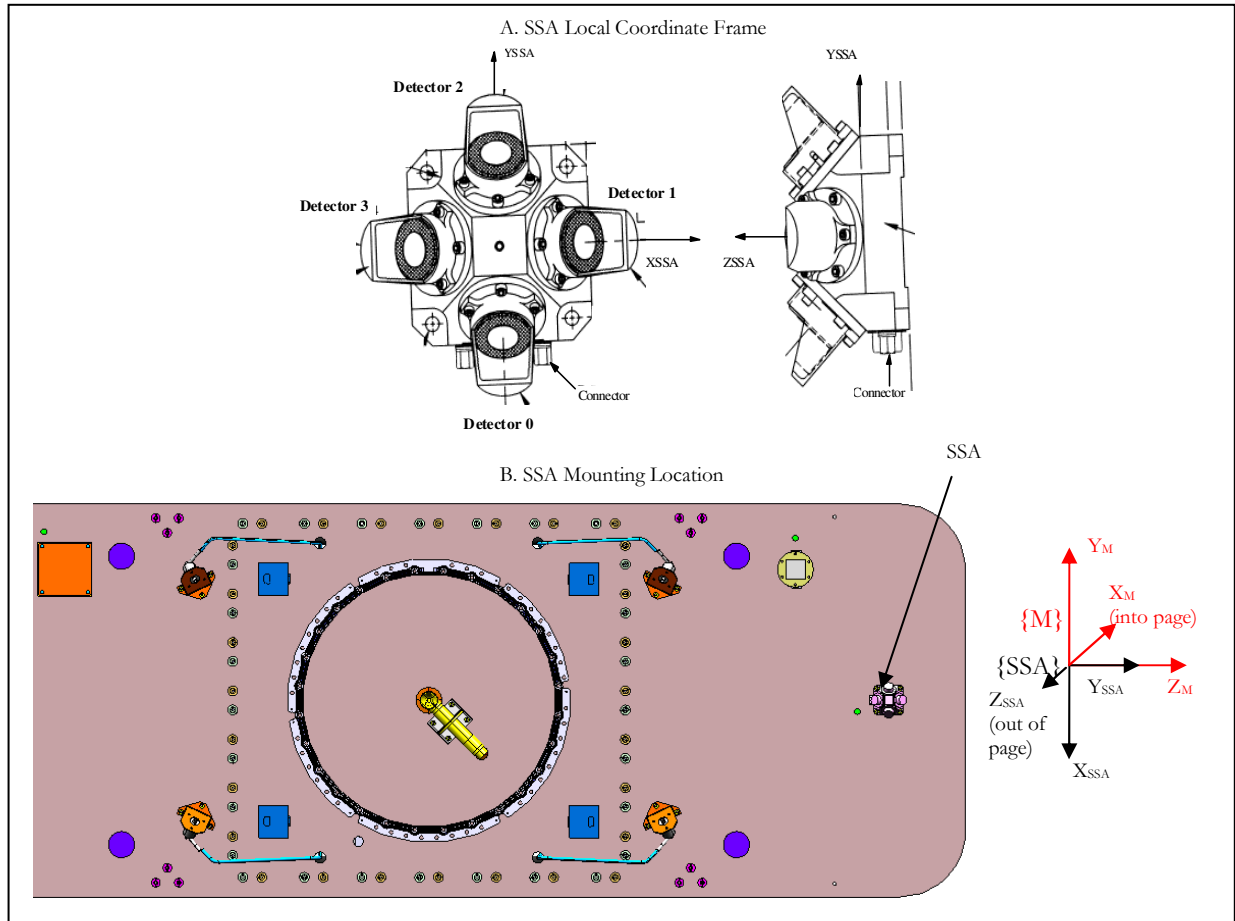


Figure 4.8 -Sun Sensor Assembly Local Coordinate Frame and Orientation (drawings taken from Phoenix Adcole SSA ICD rev E, dated 4/24/97)

There is a single sun sensor mounted on the +Z-side of the -X panel extension of each spacecraft. Each Sun sensor houses 4 detector arrays and each detector array normal is 45 deg from the mounting plane. The detector normal unit vectors in the mechanical {M} frame are listed below.

$$Detector0 = (-0.7071 \quad 0.0000 \quad -0.7071)$$

$$Detector1 = (-0.7071 \quad -0.7071 \quad 0.0000)$$

$$Detector2 = (-0.7071 \quad 0.0000 \quad 0.7071)$$

$$Detector3 = (-0.7071 \quad 0.7071 \quad 0.0000)$$

The baffles on the sun sensor faces allow the entire unit to have a field of view half angle of 80 deg. The sun sensor is mounted on the deck such that the axes of the sun sensor are rotated with respect to the spacecraft mechanical frame. The sun sensor orientation with respect to the mechanical frame has been defined as follows:

$$\begin{aligned} +X_{SSA} &= -Y_M \\ +Y_{SSA} &= +Z_M \\ +Z_{SSA} &= -X_M \end{aligned}$$

The transformation from the {SSA} frame to the {M} is as follows:

$${}_{SSA}^M T = \begin{bmatrix} 0 & 0 & -1 \\ -1 & 0 & 0 \\ 0 & 1 & 0 \end{bmatrix}$$

The transformation from the {M} frame to the {SSA} frame is the transpose of the transformation above:

$${}_{M}^{SSA} T = \begin{bmatrix} 0 & -1 & 0 \\ 0 & 0 & 1 \\ -1 & 0 & 0 \end{bmatrix}$$

5. ACS COMPONENT POSITIONS

ACS component locations in the mechanical frame {M} are listed below in Table 5.1 for GRAIL-A and

Table 5.2 for GRAIL-B. Locations are defined based on the GRAIL IDEAS model revision 8. All component locations are measured from the origin of the {M} frame to the center of each component mounting plate.

Table 5.1 - GRAIL-A ACS Component Locations

Component	Xpos (m)	Ypos (m)	Zpos (m)	Comments
RWA-1	0.888405	0.270516	-0.079074	Center of wheel base plate from {M} origin
RWA-2	0.723305	-0.270516	0.251126	Center of wheel base plate from {M} origin
RWA-3	0.913805	-0.270516	0.155274	Center of wheel base plate from {M} origin
RWA-4	0.723305	0.270516	-0.225726	Center of wheel base plate from {M} origin
IMU	0.8763	0.1143	-0.37334	Center of IMU base plate from {M} origin
STA	0.598729	0.109654	0.511684	Center of STA base plate from {M} origin
SSA	-0.00635	0.000000	0.891949	Center of SSA base plate from {M} origin

Table 5.2 - GRAIL-B ACS Component Locations

Component	Xpos (m)	Ypos (m)	Zpos (m)	Comments
RWA-1	0.888405	0.270516	-0.079074	Center of wheel base plate from {M} origin
RWA-2	0.723305	-0.270516	0.251126	Center of wheel base plate from {M} origin

RWA-3	0.913805	-0.270516	0.155274	Center of wheel base plate from {M} origin
RWA-4	0.723305	0.270516	-0.225726	Center of wheel base plate from {M} origin
IMU	0.8763	0.1143	-0.37334	Center of IMU base plate from {M} origin
STA	0.598729	0.042746	0.511684	Center of STA base plate from {M} origin
SSA	-0.00635	0.000000	0.891949	Center of SSA base plate from {M} origin

The values in Table 5.1 and are expected to change once the true locations are measured during ATLO. Component locations should be updated with future revisions of this document.

6. THRUSTER ORIENTATIONS

GRAIL-A and GRAIL-B are each equipped with 8 ACS thrusters and one main engine. The main engine is used for large delta-v maneuvers such as TCMs, LOI, etc. The ACS thrusters are used for thrust vector control during burns, small orbit phasing correction maneuvers, and reaction wheel desaturation events. They are also used for thruster based control during rate damping, Sun search and Sun point slews, etc. The ACS thrusters are coupled so that they can apply a pure torque on the spacecraft while imparting only negligible delta-v. Specific sets of 4 thrusters ideally create perfect couples about each axis in the {M} frame.

6.1 ACS THRUSTERS

The ACS thrusters are 1 N hydrazine engines. The baseline thruster configuration is shown in Table 6.1 and defined by the unit vectors and thruster nozzle locations listed in the tables that follow. Table 6.1 provides the thruster throat locations and tags each thruster with an identifier to be referenced during the GRAIL design. Table 6.2 lists the **thruster pointing vectors** and Table 6.3 lists the **thrust unit vectors**. The coordinates in Tables 6.1 through 6.3 are measured in the spacecraft mechanical {M} frame.

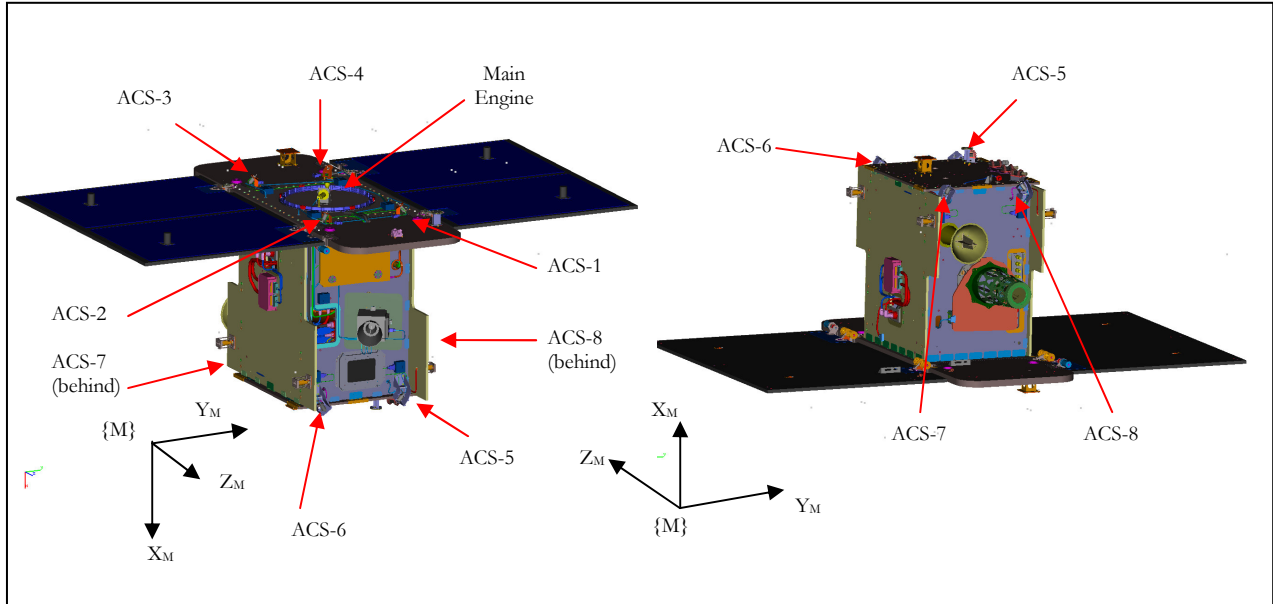


Figure 6.1 - Thruster IDs and Mounting Locations

6.1.1 Throat Positions

Table 6.1 - Thruster IDs and Throat Locations in Mechanical Frame

Thruster ID	Nozzle X Coordinate [m]	Nozzle Y Coordinate [m]	Nozzle Z Coordinate [m]
ACS-1	-0.05321	0.23643	0.45874
ACS-2	-0.05321	-0.23643	0.45874
ACS-3	-0.05321	-0.23643	-0.45874
ACS-4	-0.05321	0.23643	-0.45874
ACS-5	1.09656	0.23643	0.45874
ACS-6	1.09656	-0.23643	0.45874
ACS-7	1.09656	-0.23643	-0.45874
ACS-8	1.09656	0.23643	-0.45874

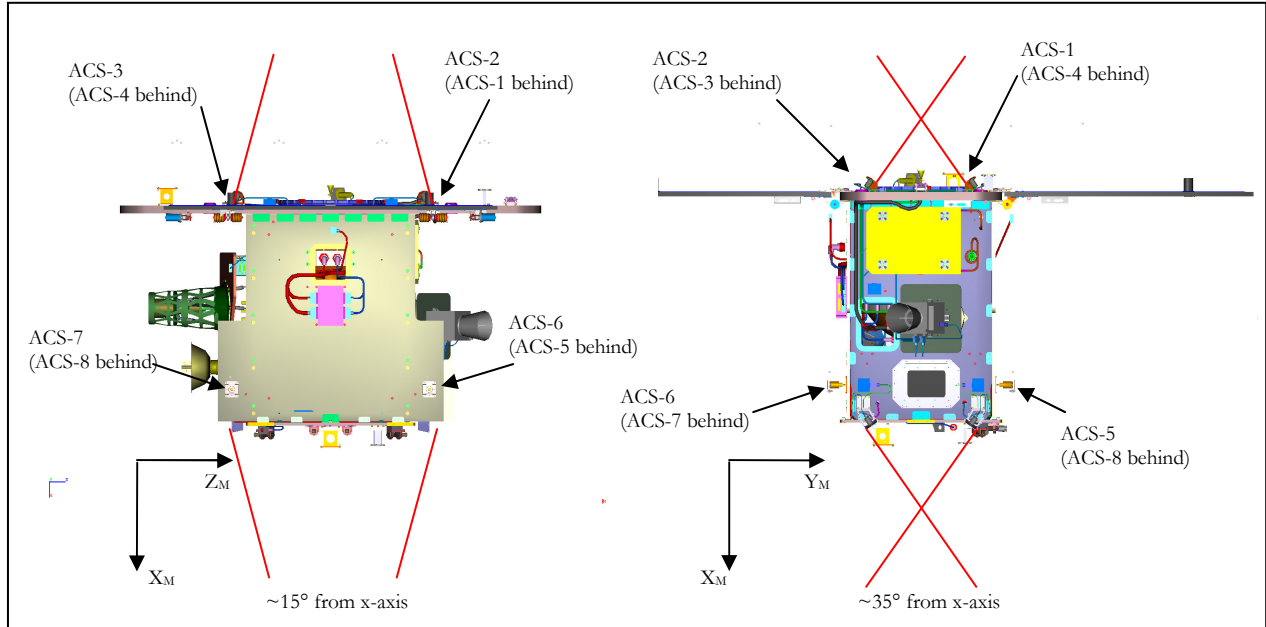


Figure 6.2 - Thruster IDs and Pointing Directions

6.1.2 Nozzle Pointing Unit Vectors

The thruster pointing directions were chosen such that when viewed in the x-z plane, the pointing vectors make approximately a 15° angle with the x-axis. When viewed from the x-y plane, the pointing vectors make approximately a 35° angle with the x-axis (as shown in Table 6.2).

Table 6.2 - Thruster Nozzle Pointing Unit Vectors [Mechanical Frame]

Thruster ID	X	Y	Z
ACS-1	-0.79124	-0.55403	-0.25882
ACS-2	-0.79124	0.55403	-0.25882
ACS-3	-0.79124	0.55403	0.25882
ACS-4	-0.79124	-0.55403	0.25882
ACS-5	0.79124	-0.55403	-0.25882
ACS-6	0.79124	0.55403	-0.25882
ACS-7	0.79124	0.55403	0.25882
ACS-8	0.79124	-0.55403	0.25882

6.1.3 Thrust Vectors

Table 6.3 - Thrust Unit Vectors [Mechanical Frame]

Thruster ID	X	Y	Z
ACS-1	0.79124	0.55403	0.25882
ACS-2	0.79124	-0.55403	0.25882
ACS-3	0.79124	-0.55403	-0.25882
ACS-4	0.79124	0.55403	-0.25882
ACS-5	-0.79124	0.55403	0.25882
ACS-6	-0.79124	-0.55403	0.25882
ACS-7	-0.79124	-0.55403	-0.25882
ACS-8	-0.79124	0.55403	-0.25882

6.2 MAIN ENGINE

The main engine consists of one 22 N thruster mounted on the $-X$ bus panel as shown in Figure 6.1.

6.2.1 Throat Position

Thruster ID	Nozzle X Coordinate [m]	Nozzle Y Coordinate [m]	Nozzle Z Coordinate [m]
Main Engine	-0.05921	0.00000	0.00000

6.2.2 Thruster Nozzle Pointing Unit Vector

Thruster ID	X	Y	Z
Main Engine	-1.00000	0.00000	0.00000

6.2.3 Thrust Vector

Thruster ID	X	Y	Z
Main Engine	1.00000	0.00000	0.00000

7. FUEL TANK

The GRAIL fuel tank is a titanium diaphragm tank used to store liquid hydrazine propellant. The tank is pictured below. Tank dimensions and location in the $\{M\}$ frame is listed in the following tables.

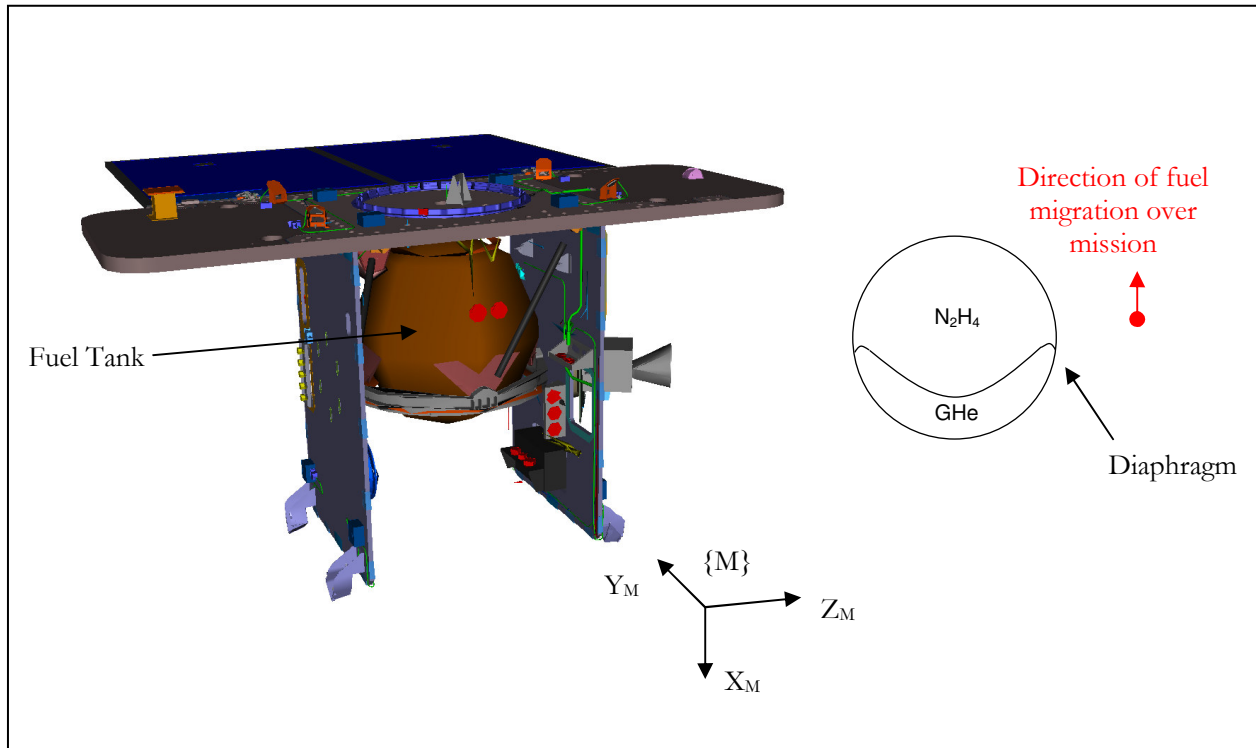


Figure 7.1 - GRAIL Fuel Tank

Table 7.1 - GRAIL Fuel Tank Dimensions and Location

Description	Measurement	Inches	Meters
Tank Location in Mechanical Frame (Center of Tank)	(X_M, Y_M, Z_M)	(15.595, 0, 0)	(0.3961, 0, 0)
Tank Dimensions – Tank shape is that of two hemispheres connected by a cylinder. Diameter shown is diameter of the cylinder. Length listed is the length from the top of one hemisphere to the other.	Internal Diameter	23.126	0.5874
	Length	25.456	0.6466
	Hemisphere Internal Radius	11.563	0.2937
	Cylinder Only length	2.330	0.0592

8. KA-BAND PAYLOAD

The Ka-band payload bore sight unit vectors and mounting orientations are referenced below due to the impact the payload has on spacecraft pointing during the science phase of the mission. During science activities, each spacecraft will be required to point its associated Ka-band payload bore sight towards the

other spacecraft so that an RF link between payloads can be established. To optimize pointing when pointing the payload bore sights toward the other spacecraft, a 2.1 deg cant is built into the payload mounting bracket. The GRAIL-A payload is canted 2.1 deg towards the $-Y_M$ axis while the GRAIL-B payload is canted 2.1 deg towards the $+Y_M$ axis as shown in Figure 8.1 below.

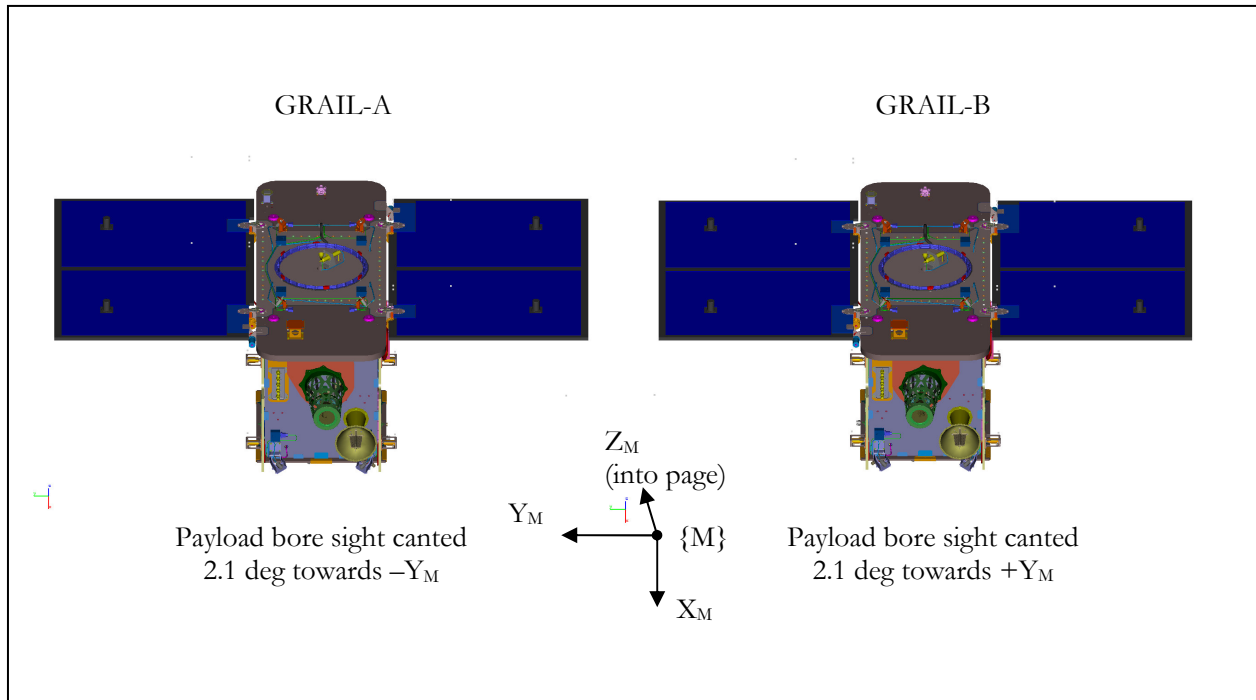


Figure 8.1 - Ka-Band Payload Bore sight Orientation

The unit vectors of the Ka-band payload bore sight for each spacecraft is shown below in the mechanical frame.

Table 8.1 - Ka-Band Payload Bore Sight Unit Vectors [Mechanical Frame]

	X	Y	Z
GRAIL-A Payload Bore Sight	0	-0.03664	-0.99933
GRAIL-B Payload Bore Sight	0	0.03664	-0.99933

9. LGA POINTING

Each spacecraft is equipped with two Low-Gain Antennas (LGA). One antenna is mounted on the $-X$ face of each spacecraft and one antenna is mounted on the $+X$ face of each spacecraft.

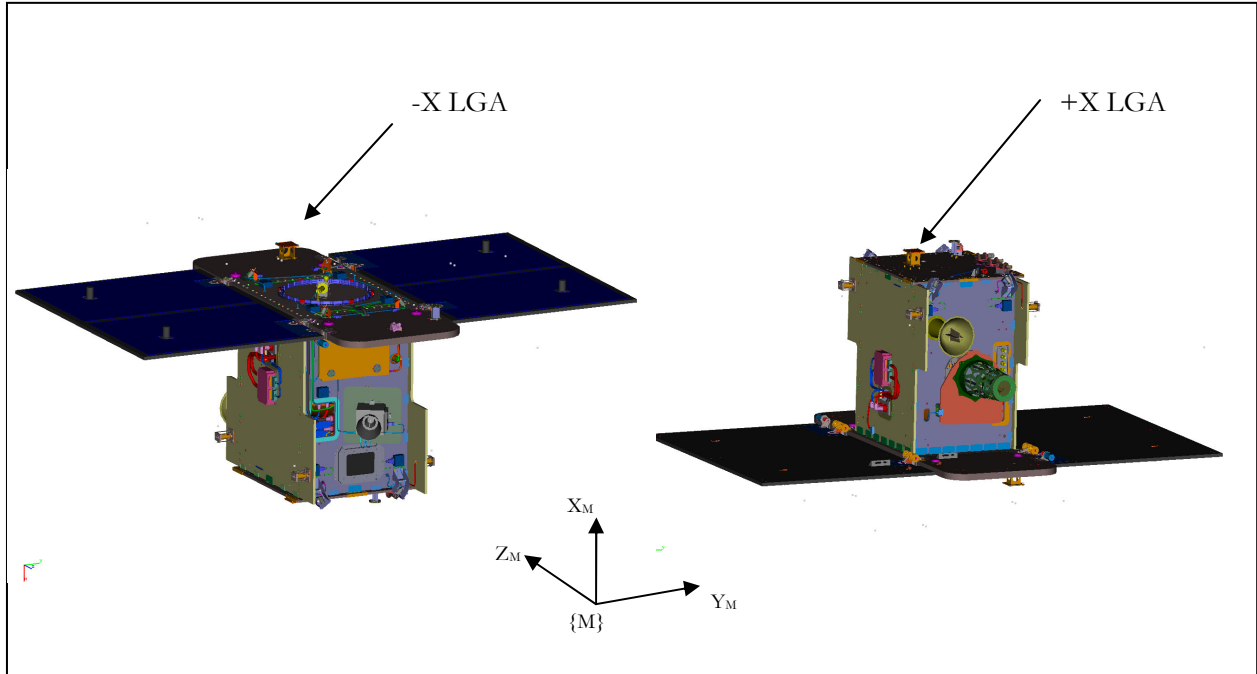


Figure 9.1 - LGA Orientation

The bore sight unit vectors for the LGAs are identical for each spacecraft. The unit vectors are shown below.

Table 9.1- LGA Bore Sight Unit Vectors [Mechanical Frame]

	X	Y	Z
+X LGA	1.0	0.0	0.0
-X LGA	-1.0	0.0	0.0

10. REVISION LOG

REV	REV DATE	AUTHOR	Revisions Made
Basic	4/23/2009	R. Olds	Original Version.
1	7/6/2009	R. Olds	Adjusted main engine and ACS thruster locations to reflect the throat positions instead of the exit plane center locations.